INTERPRETATION OF GEOCHEMICAL WELL TESTS DATA FOR OW-903B, OW-904B AND OW-909 - OLKARIA DOMES, KENYA.

Malimo, Sylvia Joan.
Geothermal Development Company.
P.O Box 100746 -00101- NAIROBI, KENYA.smalimo@gdc.co.ke

ABSTRACT

Three production wells from the Olkaria Domes field (Kenya) were allowed to discharge for 3 months in early 2009 and this communication describes the chemical composition of the fluids from these three wells (OW-903B, OW-904B and OW 909). Down hole temperatures range from 250^{o}C to 350^{o}C for these three wells which agree with the solute and gas geothermometers. The wells produce fluids with high pH, deep fluid pH ranges from 6.9 to 8.3. OW 909 has higher deep fluid TDS, pH and concentrations of anions (B, Cl, F), Na and K as compared to OW 903B and OW 904B. Olkaria Domes wells have a sodium bicarbonate water type similar to those of Olkaria west and Olkaria central fields. Concentrations of most dissolved constituents were initially low but then increased with increasing enthalpy, a considerable range in observed concentrations. Deep fluids appear to be close to equilibrium with quartz and calcite. Very low Ca concentrations suggest that calcite scaling will not be a problem for the utilization of the Olkaria Domes geothermal fluids in electricity generation but fluid has to be separated at temperatures above 100°C to prevent silica scaling. There´s also low carbon dioxide emission from these wells.

INTRODUCTION

The Greater Olkaria Geothermal Area (GOGA) is situated south of Lake Naivasha on the floor of the southern segment of the Kenya rift (Figure 1). The Kenya rift is part of the East African rift system that runs from Afar triple junction at the Gulf of Eden in the north to Beira, Mozambique in the south. It is the segment of the eastern arm of the rift that extends from Lake Turkana to the North, and to Lake Natron northern Tanzania to the south. The rift is part of a continental divergent zone where spreading occurs resulting in the thinning of the crust hence eruption of lavas and associated volcanic activities (Lagat 2004).

The Greater Olkaria Geothermal Area consists of seven sectors namely, Olkaria North East, Olkaria East, Olkaria Central, Olkaria South West, Olkaria North West, Olkaria South East and Olkaria Domes. This report concentrates on part of the Greater Olkaria Geothermal Area – the Olkaria Domes field, which is being developed by the Kenya Electricity Generating Company (KENGEN), in addition to their other two producing fields - Olkaria East and Olkaria North East. This study aims at interpreting the geothermal fluid types, the chemical components and any recommendations resulting thereof in evaluating the chemistry of well discharges from three Olkaria Domes wells (OW 903B, OW 904B and OW 909). I also compare the waters of the Domes field to the other six fields in the Greater Olkaria Geothermal Area.

BACKGROUND

General and status of development

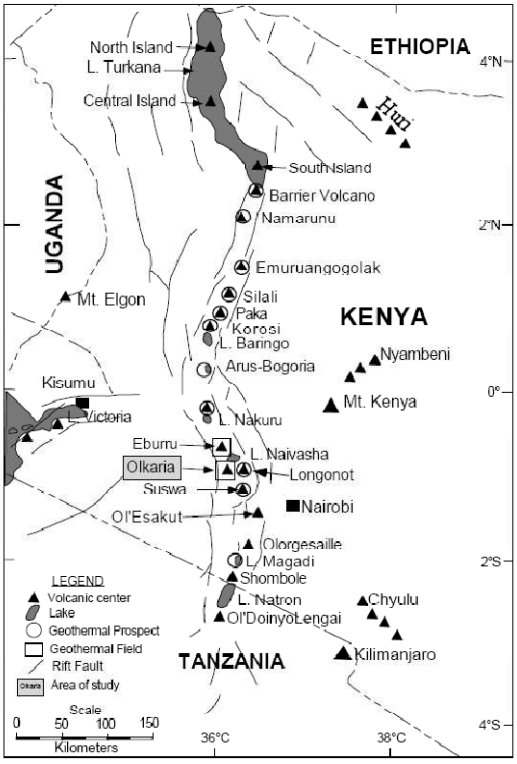

FIGURE 1: Map of the Kenya rift showing the location of Olkaria geothermal field and other quaternary volcanoes along the rift axis.

conducted and the fluids characterised. These were a mixed sodium bicarbonate–chloride–sulphate water type with very dilute chloride concentrations ranging from 178 to 280 ppm (Opondo 2008).

GEOLOGICAL SETTING

The volcanic activity in the Olkaria domes area has progressed from Miocene to the present with eruption producing rocks ranging from intermediate to acid with minor basic eruptions. Major volcanic and fissure controlled eruptions characterised by caldera collapse phases have resulted in uneven surface topography covered by fresh lava rocks and pyroclastics. Some of the volcanic centres are aligned on an arcuate structure that suggests that the Olkaria complex is a remnant of an older caldera which is commonly known as the ring structure. The presence of the ring of domes has been used to suggest the presence of a buried caldera (Mungania 1992). The surface outcrops mainly comprise alkali rhyolite lava flows, pyroclastic deposits, some trachytic and basaltic flows. Pyroclastic deposits comprise compacted and reworked beds and pumice rich deposits which are very thick on the Domes. Some lava dykes up to 6 m thick have been observed to cut across the pyroclastics a NS direction. The pyroclastic ash deposits are well layered and vary from weakly to highly weathered often imparting a brownish colour to the deposits (Omenda 1999).

Olkaria Domes Field is located within the GOGA and lies to the west of Longonot Volcano. Olkaria Domes is the latest of these seven sectors to be deep drilled. Three deep exploration wells were drilled between 1998 and 1999. An approximately 15 wells, both vertical and directional, have been drilled in the domes area (as of May 2009). Olkaria East and Olkaria North East are fully developed with installed capacities of 45 MWe and 70 MWe. Optimization for the two power plants operated by KENGEN in Olkaria East and Olkaria North East fields are underway with more wells being drilled in the Olkaria East field. Olkaria South West has a 50 MWe binary plant operated by Orpower4 Inc while a smaller binary plant of ~4 MWe is operated by Oserian Development Company (ODC).

Olkaria Domes Field lies to the east of the Olkaria East Field (Figure 2). It is bound approximately by the Hell's Gate National Park, Ol' Njorowa gorge to the west and a ring of domes to the north and south (Mungania 1999). Most of the Olkaria Domes Field lies within the less than 20 Ωm apparent resistivity zone that covers the central and western portions of the Olkaria Domes prospect. The rest of the field lies within the 30 Ωm apparent resistivity (Onacha 1993). Three initial exploration wells were sited in the Olkaria Domes Field and were drilled to depths varying from 1900m to 2200m vertical depth. These were wells OW-901, OW-902 and OW-903. These wells were sited to investigate the easterly, southerly and westerly extents of the reservoir and the structures that provide fluid flow into the field. Discharge tests were

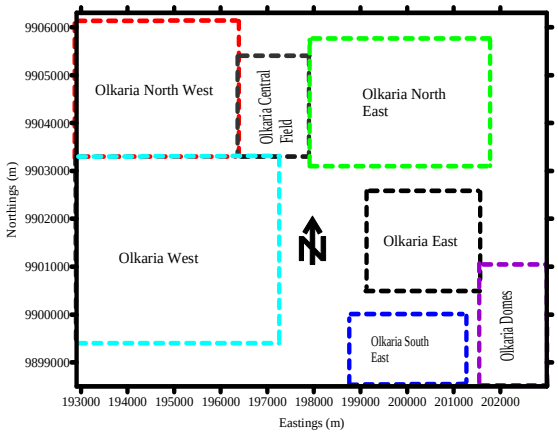

FIGURE 2: Geothermal Fields in the Greater Olkaria Geothermal Area (GOGA).

The Ol'Njorowa Gorge is probably an important structural feature that separates the Olkaria East Field from the Olkaria Domes field. Comendite is exposed in a few locations along lava fronts and along the Ol'Njorowa gorge. The rocks consist of unconsolidated pyroclastics, alkali rhyolite lavas with intercalations of tuffs, basalts interstratified with trachytes and synetitic intrusives at the bottom of the wells (Mungania 1999; Omenda 1999). The eruptive material covering Olkaria volcanic complex area is characterised by acid pyroclastics and alkali rich lavas to an elevation of about 1400 m.a.s.l. The high concentrations of incompatible trace elements imply that the volcanic activity tapped the upper parts of a highly fractionated magma reservoir rich in volatiles.

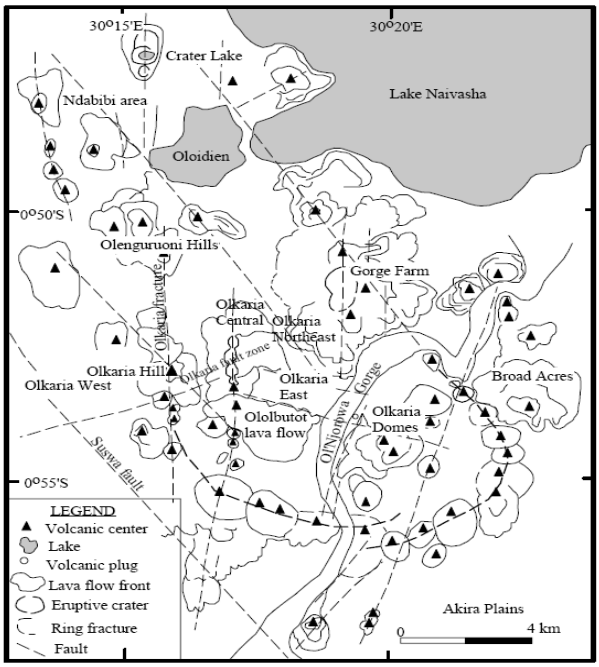

FIGURE 3: Volcano-tectonic map of the Greater Olkaria volcanic complex (modified from Clarke et al., 1990).

This is further supported by the presence of gas charged magmatic products like pumice and features of explosive volcanism like craters and caldera. According to Clarke et al., 1990, xenoliths of syenite in pyroclastics within the Domes and Longonot areas imply a possible cold or cooling upper part of a magma body which is interpreted to be shallower towards Longonot. The zone between 1400 m.a.s.l and 1000 m.a.s.l is dominated by thin basaltic and pyroclastics flows indicating quiet fissure eruptions and a period of strombolean type volcanism. Below 1000 m.a.s.l, trachytic lava dominates with associated pyroclastics and basalts. The trachytes are further divided into two types. The first is a quartz rich porphyritic type that extends to an elevation of 500 and may represent the remnant of the Olkaria mountain shield lavas. The second is a fine grained type having flow texture may indicate low viscosity associated with Pliocene plateau lavas.

Starting from these plateau lavas, the following volcanological model, (Figure 4), was first put forward:

a) The old Pliocene volcanic terrain covered by flood volcanics is characterised by block faulting associated with extensional tectonics.
b) The Plio-pleistocene shield volcano was built upon the shield quartz-trachyte lavas. The volcano then collapsed and formed a cauldron floor at about 1000 – 1200 m.a.s.l and due the emptying of the volatile rich parts, of the magma chamber during the explosive caldera collapse phase, more basic magma erupted effusively into the cauldron floor.
c) Reactivation of N-S faults during Pleistocene caused further explosive withdrawal of magma from a deep differentiated magma chamber. This phase may have been contemporaneous with activity in Longonot. (Onacha and Mungania 1993.)

Previous work.

Detailed geological, geophysical and geochemical work was conducted in the area by different workers (Mungania 1992). The surface exploration with emphasis in the Olkaria Domes field was conducted in the period 1992 to 1993 for geophysical, geological and geochemical surveys. This led to the development of a basic working model that resulted in recommendations to drill three wells. Exploration drilling started in June 1998 through June 1999 and three wells drilled to completion. Three geothermal exploration wells OW-901, OW-902 and OW-903 were drilled in Olkaria Domes field to evaluate its geothermal potential. The three wells (Figure 5) were drilled to a depth of 2200 m and all encountered a high temperature system and discharged on test. The highest recorded measured temperatures in the wells were; 342°C at -

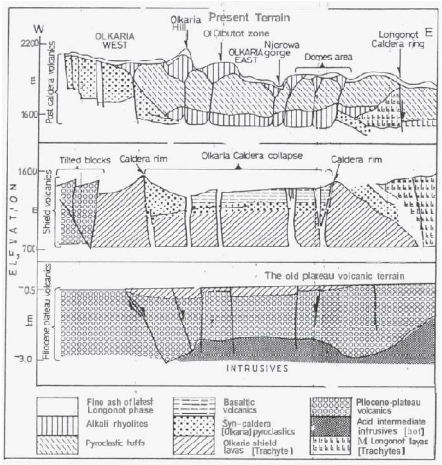

FIGURE 4: Volcanological model of Olkaria Domes area.

290 m.a.s.l, 248°C at 207 m.a.s.l and 341°C at -107m.a.s.l for wells OW-901, OW-902 and OW-903 respectively. Rocks encountered in the wells include pyroclastics, rhyolite, tuff, trachyte, basalt and minor dolerite and microsyenite intrusives.

Fractures, vesicles, spaces between breccia fragments, glassy rocks and primary minerals exhibit little or no hydrothermal alteration in the upper parts of the wells with mainly silica, calcite, zeolites, phyllosilicates, oxides and sulphides being the alteration minerals present. In the deeper parts of the wells, however, hydrothermal alteration to ranged from high to extensive. Hydrothermal zeolites, calcite, epidote, phyllosilicates, silica, sulphides, epidote, albite, adularia, biotite, garnet, fluorite, prehnite, oxides and titanite are the alteration minerals observed. The most important hydrothermal alteration controls in Olkaria Domes field are temperature, rock types and permeability (Lagat 2004).

FIGURE 5. Domes map showing the location of wells.

Four hydrothermal alteration zones were recognized in the field based on the distribution of the hydrothermal alteration minerals. They are in the order of increasing depth and temperature; the zeolite-chlorite, the illite-chlorite, the illite-chlorite-epidote and the garnet-biotite-actinolite zones. Feeder zones in the wells were found to be confined to faults, fractures, joints and lithologic contacts. Observations from hydrothermal alteration mineralogy, pressure and temperature profiles indicate that well OW-901 is close to the upflow whereas well OW-903 is in the outflow zone and well OW-902 is in the outflow and also the marginal zone of the field. The geochemical analysis found a mixed type sodium bicarbonate-chloride-sulphate water with dilute chloride concentration (chloride ~178-280 ppm). The pH of fluids discharged tended to be alkali (8.68 to 10.69) as sampled at atmospheric pressure and analysd at room temperature (25°C). Carbon dioxide gas concentration in steam, on average, was high relative to that of the Olkaria East Field. A less mineralised water component was found to exist in this field. Solute geothermometry offered a good estimate of temperatures where dilute fluids inflow into the wells between 1000m to 1200m. Gas geothermometry approximated to the deep temperature in the reservoir though these were less than measured temperatures at well bottom (Opondo 2008).

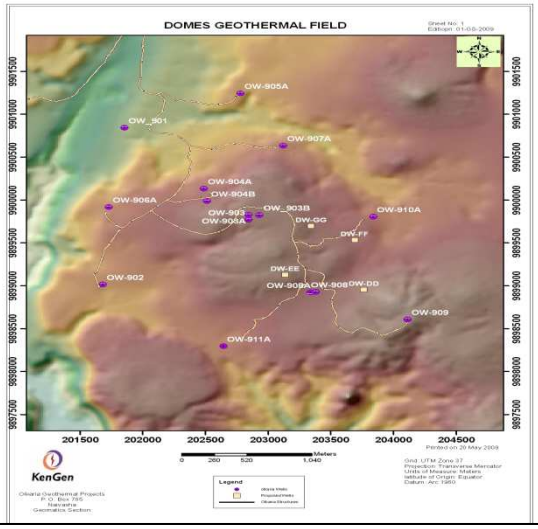

FIGURE 5: Domes map showing the location of wells.

Geology of OW 903B, OW 904B and OW 909

The major rock types found during drilling were trachytes with occurrences of epidotes and basalts for the three wells selected for this study. Trachytes dominate from shallow depths with secondary minerals of clays and pyrites. Basalts and tuffs were also observed in the drill cuttings with dominating clay, pyrite and calcite as the secondary minerals.

Reservoir temperature and pressure profiles

For the selected three wells from the Olkaria domes, the specifications of the wells are listed in Table 1. Figure 7 shows the temperature logs of the domes wells for different times during heating, injection and shut in. From these logs, I was able to choose reference temperatures that are necessary for computing deep fluid compositions from two phases chemical analyses.

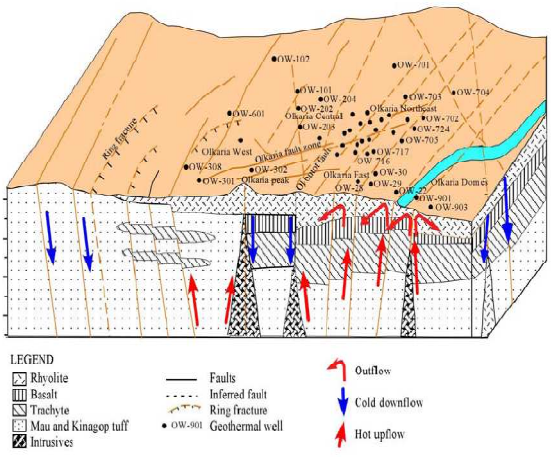

FIGURE 6: A conceptualized geological model of the Greater Olkaria Geothermal Area showing generalized geology and the locations of the fields with respect to downflow, upflow and the outflow zones. (Lagat, 2004)

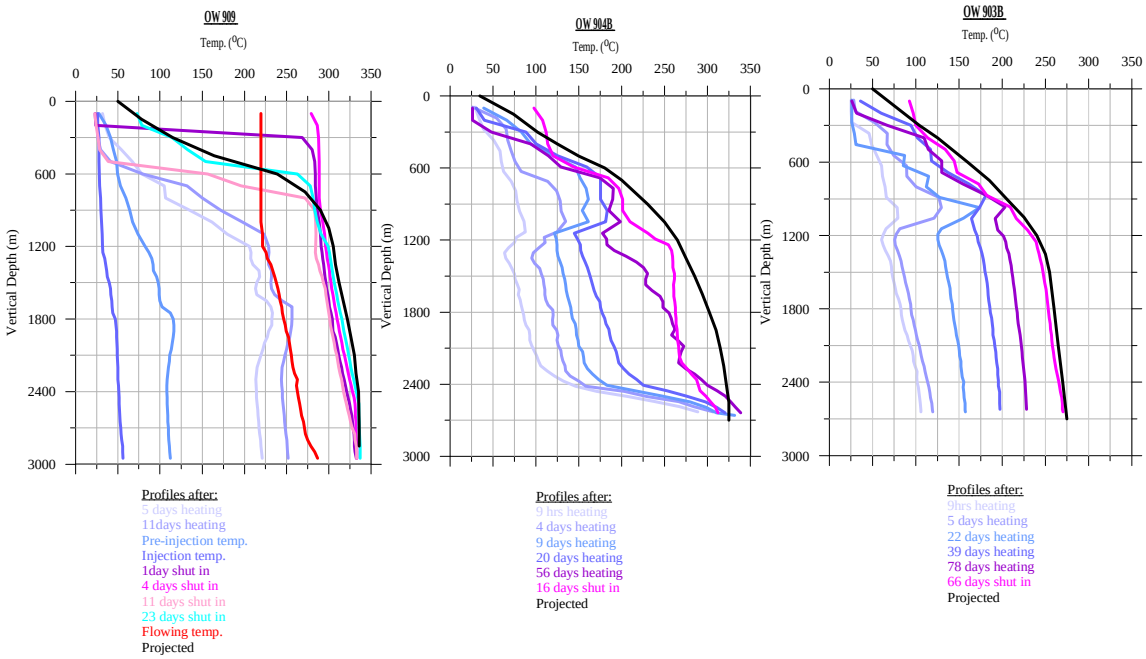

FIGURE 7. Temperature profiles of Olkaria Domes wells

Well	Type	Drilled Depth (m)	Production Casing Depth (m)	Reference temperature (°C)
OW 903B	Directional	2800	1200	250
OW 904B	Directional	2820	1200	260
OW 909	Vertical	3000	1200	300

TABLE 1: Well information

GEOCHEMICAL DATA AND TRENDS

Sampling and analysis

Water chemistry data is essential information required for the characterization of geothermal fluids and evaluation of energy potential of geothermal fields by geothermometry, and provides good indicators for monitoring reservoir changes in response to production and also allow us to evaluate and avoid scaling problems in wells and surface pipelines. Analytical results with good quality are the key to accurately evaluating geothermal resources and effectively solving reservoir management problems. Collection of samples for chemical analysis is the first step in a long process which eventually yields results that provide information that is used to answer different geochemical questions. In this study two-phase fluid samples from three discharging wells, OW 903B, OW 904B and OW 909 are considered. Steam samples were collected using the Webre separator on the wellhead while the liquid samples were collected at the weir box of the silencer. The liquid samples were collected in plastic bottles while the vapour samples were collected in evacuated double port glass bottles (Giggenbach flasks) containing 50ml of 40% NaOH. According to Ármannsson and Ólafsson 2006, different ways can be used to preserve the samples. Onsite analysis for H_2S in the water samples, acidification for cations and dilution for silica samples was done. The samples were then analysed for

the different elements and gases. Analytical methods for individual components in liquid samples are shown in Table 2. All the gases (CO_2, H_2S, CH_4, H_2, and N_2) were analysed using gas chromatography.

TABLE 2: Methods used for analysis of different elements in collected samples (Pang and Armannsson 2006).

Analysis for:	Method
a. pH	- pH meter
b. Conductivity / TDS	- Conductivity meter / gravimetry
c. CO_2	- Titrimetry
d. H_2S	- Titrimetry
e. B	- Spectrometry
f. SiO_2	- Spectrophotometry (with ammonium- molybdate)
g. Na	- AAS
h. K	- ISE
i. Mg	- AAS
j. Ca	- AAS
k. F	- ISE
l. Cl	- Spectrophotometry with thiocyanate
m. SO_4^{2-}	- Turbidometry with barium chloride

Results

The three selected wells in the domes area of the Olkaria geothermal field were sampled and tested for a period of about 5 months i.e. from February to June 2009. See data appendices I and II. From reservoir measurements, the enthalpy remained constant at about 2000 kJ/Kg while the discharge rates were as follows: steam discharge increased from 37 t/hr to 50 t/hr while water discharge was constant at ranges of 20 t/hr to 30 t/hr. A total of 88 samples were collected. The tables in appendix I show the raw water and gas data. Most of the samples from the wells had no detectable magnesium and the calcium concentrations were low (less than 10ppm).

In order to compute the deep fluid composition from the liquid sample (collected at atmospheric pressure) and the steam sample (collected at 1.2 to 7 bars) it was necessary to recalculate the steam sample composition to atmospheric pressure. The atmospheric steam composition was combined with the liquid sample composition in the computation of the deep fluid composition using the WATCH programme Version 2.1 (Arnórsson and Bjarnason 1994). Samples with good ionic charge balance (charge balance from -10 to +10) were then speciated using the WATCH program to give concentration of the deep fluids (Appendix II). For any solution, the total charge of positively charged ions will equal the total charge of negatively charged ions in reality. The net charge for any solution must equal zero. In the samples analyzed, though, the charge balances were not = 0 so the samples with the closest charge balance, i.e. ±10, were used.

GEOCHEMICAL DATA INTERPRETATION

Trends with time in the composition of well discharges

A total of 88 samples were used to compute the trends of the three wells sampled during discharge. The different solute and gas components were monitored and sampled to evaluate the recovery of the wells after shut in. Appendix shows the trends in the different components monitored for a period of about 100 days. OW 909 seems to have higher concentrations of the cation components as compared to OW 903B and OW 904B. Despite the limited time of recovery, the sulphate concentrations are declining with time as the H_2S concentrations increase showing good geothermal water inflow into the wells. The scatter in the data might in part result from non-equilibration of the geothermal water and the drilling fluids that had not totally been discharged from the wells and to some degree it might reflect analytical uncertainties.

Correlation of discharge components with chloride

Plots depicting the concentrations of several components such as B, SiO_2, Ca, Na, K and F as a function of Cl concentration are shown in appendix III. These plots seem to indicate that the ratios of chloride are close to linear with the other components except with calcium which is in very low concentrations in these new wells. This indicates that there is still mixing of the cold and hot water in the upflow. The concentrations of dissolved constituents in the fluids from wells OW 904B and OW 903B tend to be very similar whereas the fluids from well OW 909 tend to have higher concentrations of dissolved solids.

Cl-SO_4-HCO_3 ternary diagram

According to Giggenbach 1991, ternary diagrams are used for the classification of thermal water based on the relative concentrations of the three major anions Cl^-, SO_4^{2-} and HCO_3^-. Chloride, which is a conservative ion in geothermal fluids, does not take part in reactions with rocks after it has dissolved. Chloride, does not precipitate after it has dissolved; its concentration is independent of the mineral equilibria that control the concentration of the rock-forming constituents. Thus, chloride is used as a tracer in geothermal investigations. The Cl-SO_4-HCO_3 ternary diagram is one diagram for classifying natural waters (Giggenbach, 1991). Using this diagram, several types of thermal water can be distinguished: mature waters, peripheral waters, steam-heated waters and volcanic waters. The diagram provides an initial indication of mixing relationships. According to Giggenbach 1991, the chloride-rich waters are generally found near the upflow zones of geothermal systems. High SO_4^{2-} steam-heated waters are usually encountered over the more elevated parts of a field. Degree of separation between data points for high chloride and bicarbonate waters may give an idea of the relative degree of interaction of the CO_2 charge fluid at lower temperature, and of the HCO_3^- concentration increased with time and distance travelled underground.

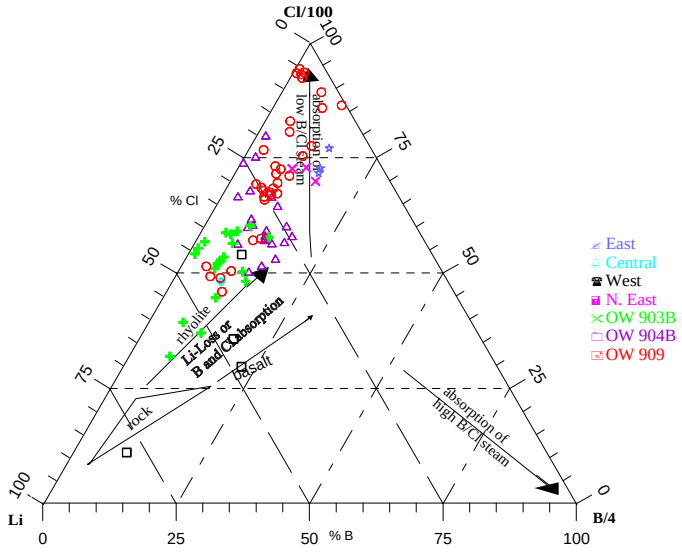

FIGURE 9: Comparative plot of relative Cl, Li, and B from wells in

Figure 8 shows that the three Olkaria Domes wells (OW 903B, OW904B and OW909) plot in the region with high HCO_3 peripheral waters with low chloride. This illustrates that the geothermal fluids in the Olkaria Domes reservoir are bicarbonate waters and correspond to peripheral waters (Giggenbach, 1991). The figure also shows the correlation of the waters with those of the other fields in the GOGA. The Olkaria Domes fluids seem to plot similar to those of Olkaria west and Olkaria central fields. From the relative abundance of chloride, sulphate and bicarbonate of the Olkaria wells, these waters would be classified as sodium-chloride and sodium-bicarbonate water, or mixtures thereof (Figure 8). Wells in the Olkaria East production field and in Olkaria Northeast discharge sodium-chloride type water that are classified as more mature according to the scheme of Giggenbach 1991.

Relative Cl, Li and B contents

Lithium is used as a tracer, because it is the alkali metal least affected by secondary processes for initial deep rock dissolution and as a reference for evaluating the possible origin of two important 'conservative' constituents of geothermal waters, Cl and B. Once added, Li remains largely in solution. The B content of thermal fluids is likely to reflect to some degree the maturity of a geothermal system; because of its volatility it is expelled during the early heating up stages. In such a case, fluids from older hydrothermal systems can be expected to be depleted in B while the converse holds for younger hydrothermal systems. It is, however, striking that both Cl and B are added to the Li containing solutions in proportions close to those in crustal rocks. At higher temperatures Cl occurs as HCl and B as H_3BO_3. Both are volatile and able to be mobilized by high temperature steam. They are, therefore, quite likely to have been introduced with the magmatic vapour invoked above to lead to the formation of deep acid brine responsible for rock dissolution (Karingithi 2000).

At low temperatures the acidity of HCl increases rapidly, and is soon converted by the rock to the less volatile NaCl. B remains in volatile form to be carried in the vapour phase even at lower temperatures. The Cl/B ratio is often used to indicate a common reservoir source for the waters. Care must however, be taken in applying such interpretation since waters from the same reservoir may show differences in this ratio, due to changes in lithology at depth over a field (example, the occurrence of a sedimentary horizon), or by the absorption of B into clays during lateral flow.

The fluid discharges from Olkaria Domes wells (OW-903B, OW-904B and OW-909) plot in the region along the Li-Cl axis but do not cluster around the same point. B/Cl ratios are in the intermediate region and could suggest the absorption of low B/Cl magmatic vapours. Discharges from the Olkaria –Domes wells show comparatively low lithium content. This is also shown in the other well discharges from the other GOGA wells. See figure 9.

Geothermometry

Chemical geothermometers are based on the assumption that temperature dependent mineral solute equilibrium is attained in the geothermal reservoir. In this report chemical geothermometers are used to assess the reservoir temperatures for the three wells chosen from Olkaria Domes. Studies indicate that geothermal water compositions are controlled by a close approach to mineral-solution equilibria with respect to various elements (Arnórsson et al., 1983a; Tole et al., 1993; Karingithi, 2000). Changes, which occur in temperature and water composition during boiling between aquifer and wellhead, generally lead to changes in mineral saturation. Such changes may result in mineral precipitation or mineral dissolution. Together with physical processes in the depressurization zone around wells, these changes may cause well discharge compositions to differ from the chemical composition of the aquifer fluid.

Solute Geothermometers

In geochemical studies, water chemistry and gas composition of geothermal fluids have proved useful in assessing the characteristics of geothermal reservoirs, both to estimate temperatures (Arnórsson and Gunnlaugsson, 1983; D'Amore and Truesdell, 1985) and to estimate initial steam fractions in the reservoir fluid (D'Amore and Celati, 1983; D'Amore and Truesdell, 1985).

The following solute geothermometers are used in this study:

Quartz - Fournier (1977)
- Fournier and Potter (1982)
- Fournier (1979)

Na-K - Arnórsson et al. (1983)
- Giggenbach (1988)

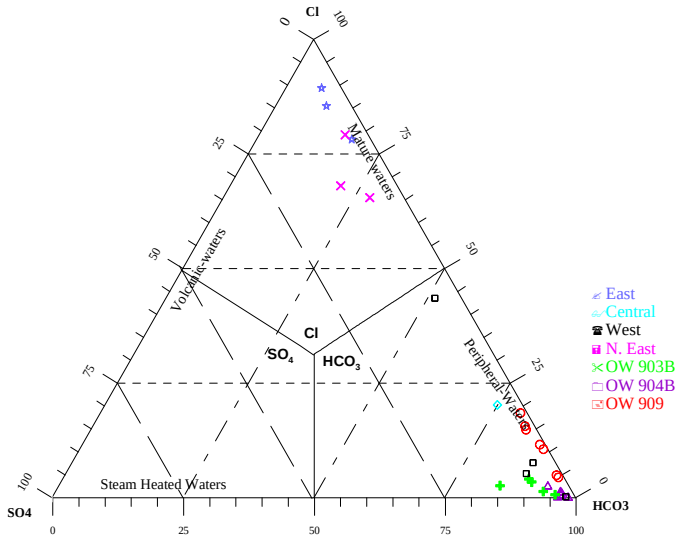

FIGURE 8: Comparative plot of relative Cl-SO4 -HCO3 contents from the discharges of wells in the GOGA fields.

Silica geothermometers

The silica geothermometers are based on experimentally determined solubilities of chalcedony and quartz. Usually the quartz geothermometer is applied to high-temperature reservoirs like the Olkaria geothermal field. Application of the silica geothermometers is based on the fact that the activity of dissolved silicic acid, H_4SiO_4, in equilibrium with quartz, is temperature dependent. The solubility reactions for silica minerals can be expressed as:

$$SiO_{2,solid} + 2H_2O = H_4SiO_4{}^o \quad (1)$$

However $H_4SiO_4{}^0$ is not only aqueous silica species in natural waters. $H_4SiO_4{}^0$ is a weak acid which dissociates, if pH of the fluid is high enough to yield $H_3SiO_4{}^-$:

$$H_4SiO_4{}^0 = H^+ + H_3SiO_4{}^- \quad (2)$$

Analysis of silica in aqueous solution yields the total silica concentration, generally expressed as ppm SiO_2, which includes both un-ionized $H_4SiO_4{}^0$ and ionized ($H_3SiO_4{}^-$). The dissociation constant for silicic acid is about 10^{-10} at 25°C. Thus, at a pH of 10 ($H^+ = 10^{-10}$) the concentration of unionized silica equals that of ionized silica:

$$K_{H_4SiO_4{}^\circ} = \frac{[H^+][H_3SiO_4{}^-]}{[H_4SiO_4{}^\circ]} \quad (3)$$

When using quartz geothermometers, some factors should be considered (Fournier and Potter, 1982):

- The temperature range in which the equations are valid;
- Possible polymerization or precipitation of silica before sample collection;
- Possible polymerization of silica after sample collection;
- Control of aqueous silica by solids other than quartz;
- The effect of pH upon quartz solubility; and
- Possible dilution of hot water with cold water before the thermal waters reach the surface.

The quartz geothermometers used to estimate the aquifer temperatures in this report are:

Fournier (1977)

$$t\,(°C) = \frac{1309}{5.19 - logS} - 273.15 \quad (4)$$

Fournier and Potter (1982)

$$t(°C) = -42.2 + 0.28831S - 3.6686 \times 10^{-4}S^2 + 3.1665 \times 10^{-7}S^3 + 77.034logS \quad (5)$$

The results for the quartz calculations are shown in Table 3.

Cation geothermometers

Reactions between alkali feldspars and Na and K in aqueous solution have often been described as exchange reactions. At the temperature prevailing in geothermal systems, the reaction involves simultaneous equilibrium between Na^+ and K^+ in solution and quite pure albite and K-feldspar.

The reaction is expressed as:

$$NaAlSi_3O_8 + K^+ = KAlSi_3O_8 + Na^+ \quad (6)$$

The equilibrium constant, $K_{eq,}$ for reaction 4 is:

$$K_{eq} = \frac{[KAlSi_3O_8][Na^+]}{[NaAlSi_3O_8][K^+]} \quad (7)$$

The activities of the solid reactants are assumed to be unity and the activities of the dissolved species are about equal to their molal concentrations in aqueous solution.

Equation 5 reduces to:

$$K_{eq} = \frac{[Na^+]}{[K^+]} \quad (8)$$

In this report the following equations are used for calculating reservoir temperatures based on the Na/K activity ratio in the geothermal fluid:

Fournier (1979)

$$\mathbf{t}(℃) = \frac{\mathbf{1217}}{\mathbf{1.438 + \log(Na/K)}} - \mathbf{273.15} \quad (9)$$

Na/K temperature in the range of temperatures 250-350^{o}C (Arnórsson et al., 1983) given by:

$$\boldsymbol{t}(℃) = \frac{\mathbf{1319}}{\mathbf{1.699 + \log(Na/K)}} - \mathbf{273.15} \quad (10)$$

Na/K temperature by Giggenbach (1988) given by:

$$\boldsymbol{t}(℃) = \frac{\mathbf{1390}}{\mathbf{1.750 + \log(Na/K)}} - \mathbf{273.15} \quad (11)$$

The reference temperatures chosen agree with the different chosen geothermometers. OW 903B has aquifer temperatures in the range of 220°C to 260°C; OW 904B has temperatures in the range of 230°C to 300°C while OW 909 temperatures are in the range of 250°C to 340°C indicating good production temperatures. The results for the calculations are shown in Table 3.

Gas geothermometers

Studies in many high-temperature geothermal fields (> 200°C) indicate that the concentrations (or ratios) of gases like CO_2, H_2S, H_2, N_2, NH_3, and CH_4 are controlled by temperature-dependent gas-gas and/or mineral-gas equilibria (D'Amore and Arnórsson, 2000). On this basis, data from chemical analyses of those gases have been used to develop relationships between the relative gas concentrations and the temperature of the reservoir. Such relationships are known as *gas or steam geothermometers*. Gas geothermometers are also based on certain chemical reactions between gaseous species and minerals which are considered to be in chemical equilibrium. For each chemical equilibria considered, a thermodynamic equilibrium constant may be expressed in terms of temperature, in which case the concentration of each gas species is often represented by its partial pressure in the vapour phase (D'Amore and Truesdell, 1985).

Geothermal gases are introduced into geothermal fluid with recharge water, from water-rock interaction in the reservoir or from magmatic fluid invasion. In an undisturbed reservoir, reactions in equilibrium at the reservoir temperature control the concentrations of these gases. On boiling, the partitioning of gases between liquid and vapour phase is controlled by the enthalpy of the geothermal fluid and the boiling temperature in cases where the vapour

travels without hindrance to the surface (in boreholes and wide open fissures), negligible changes in the gas concentrations and ratios will occur, and these can be used as gas geothermometers. There are essentially three types of gas geothermometers. The first group is based on gas-gas equilibria. The second group is based on mineral-gas equilibria involving H_2S, H_2 and CH_4 but assuming CO_2 to be externally fixed. The third group is based on mineral-gas equilibria. The first two groups of geothermometers require only data on the relative abundance of gaseous components in the gas phase, whereas the third group calls for information on gas concentrations in steam (D'Amore and Arnórsson, 2000).

When using gas geothermometry, it is important to keep in mind that several factors other than aquifer temperature may affect the gas composition of a geothermal fluid. In geothermal reservoir fluids, gas concentrations at equilibrium depend on the ratio of steam to water of that fluid, whereas the gas content of fumarole steam is also affected by the boiling mechanism in the upflow, steam condensation and the separation pressure of the steam from the parent water. Furthermore, the flux of gaseous components into geothermal systems from their magmatic heat source may be quite significant and influence how closely gas-gas and mineral-gas equilibria are approached in specific aquifers (D'Amore and Arnórsson, 2000). In this study, the gas geothermometers used are those based on gas concentrations in mmol/kg corrected to the atmospheric pressure. The geothermometers are based on mineral gas equilibria and the temperature equations for the thermodynamic data for the following reactions:

$$2Ca_2Al_3Si_3O_{12}(OH) + 2CaCO_3 + 3SiO_2 + 2H_2O = 3Ca_2Al_2Si_3O_{10}(OH)_2 + 2CO_{2,aq} \quad (12)$$

$$FeS_2 + FeS + 2Ca_2Al_2Si_3O_{10}(OH)_2 + 2H_2O = 2Ca_2Al_2FeSi_3O_{12}(OH) + 3H_2S_{aq} \quad (13)$$

$$4FeS + 2Ca_2Al_2Si_3O_{10}(OH)_2 + 2H_2O = 2Ca_2Al_2FeSi_3O_{12}(OH) + 2FeS_2 + 3H_{2,aq} \quad (14)$$

Q in the gas geothermometry equations represents the gas concentrations in log mmol/kg. The equations, Arnórsson 1998, were:

For T_{CO_2}:

$$\mathbf{t}(℃) = \mathbf{4.724Q^3 - 11.068Q^2 + 72.012Q + 121.8} \quad (15)$$

T_{H_2}:

$$\boldsymbol{t}(℃) = \mathbf{6.630}\boldsymbol{Q^3} + \mathbf{5.836}\boldsymbol{Q^2} + \mathbf{56.168}\boldsymbol{Q} + \mathbf{227.1} \quad (16)$$

T_{CO_2/N_2}:

$$\boldsymbol{t}(℃) = \mathbf{1.739}\boldsymbol{Q^3} + \mathbf{7.599}\boldsymbol{Q^2} + \mathbf{48.751}\boldsymbol{Q} + \mathbf{173.2} \quad (17)$$

The results in the table 3 below show the different geothermometer results found for the three wells. The samples used to calculate for the geothermometers are those that had all the elemental analysis , the samples used to calculate the geothermometers had been discharged for a while to give a good indication of the reservoir fluid and good charge balances per well were also considered.

Well	T_{q-1}	T_{q-2}	T_{NaK-1}	T_{NaK-2}	T_{NaK-3}	T_{qtz}	T_{NaK}	T_{CO2}	T_{H2}	$T_{CO2/N2}$	$T_{ref.}$	$T_{av.}$	T_{median}
OW903B	232	238	263	248	265	249	245	221	239	259	250	246	248
OW904B	254	266	271	255	272	276	307	244	228	263	260	263	263
OW909	274	294	339	351	332	264	340	253	300	268	300	301	300

TABLE 3: Various solute and gas geothermometers of Olkaria Domes Wells.

T_{q-1}	Fournier 1977	T_{q-2}	Fournier and Potter 1982
T_{NaK-1}	Fournier 1979	T_{NaK-2}	Arnórsson et al 1983

T_{NaK-3}	Giggenbach et al 1988	T_{qtz}	WATCH calculated quartz
T_{NaK}	WATCH calculated Na-K	T_{ref}	Observed temperatures
$T_{av.}$	Average Temperature	T_{median}	Median Temperature
TCO_2, TH_2, TCO_2/N_2	Arnórsson (1998)		

Deep fluid species, Log Q/K and saturation indices

As previously stated in the geothermometry section above, WATCH program was used to speciate for the deep fluids. Quartz in the deep fluids shows a slight undersaturation with a bit of scatter due to non-equilibration of the deep fluids and the drilling fluids during the discharge testing. The initial discharge samples are quite varied as compared to the later sampled ones which show equilibration with the quartz species. For the calcite deep fluid species, both the WATCH and SOLVEQ programs were used to speciated the samples. The SOLVEQ program was used to compute for the calcite because WATCH results always predicted super saturation that was not a realistic result for nature. With SOLVEQ, we get a more realistic result because it incorporates more Ca bearing species like $CaCl^+$, $CaCl_{2\ (aq)}$, CaF^+, and $Ca(HSiO_3)^+$ apart from the ones that both the programs incorporate (Ca_2^+, $CaSO_{4(aq)}$, $CaHCO_3^+{}_{(aq)}$ and $CaOH^+$).

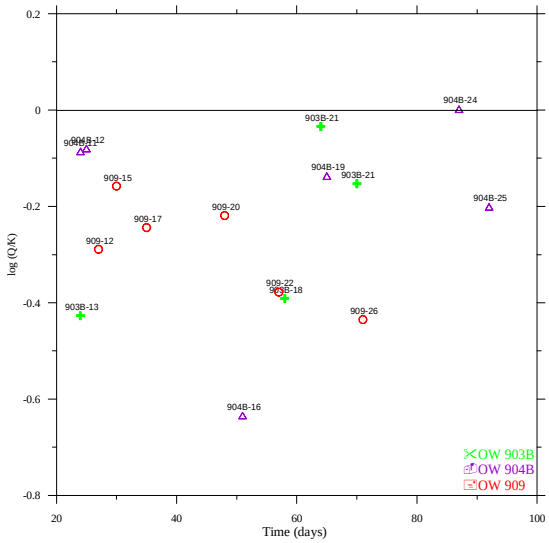

FIGURE 10: Quartz saturation of the deep fluids from Olkaria Domes field.

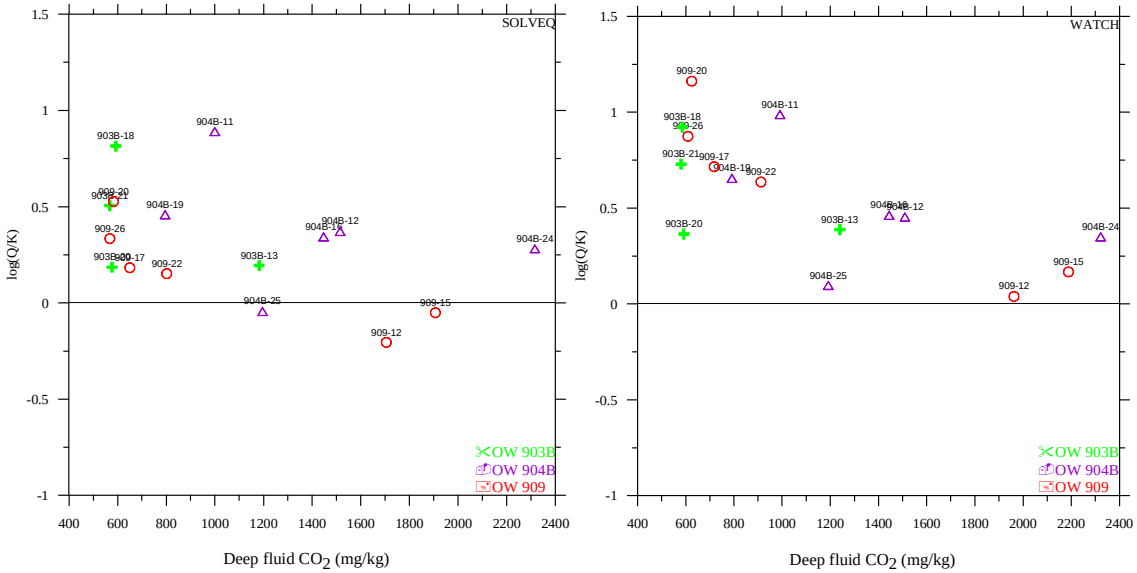

FIGURE 11: Calcite saturation of deep fluids from Olkaria Domes field.

Using the results of the aqueous speciation calculations, the saturation indices (SI) of minerals in aqueous solutions at different temperatures were computed. The SI value for each mineral is a measure of the saturation state of the water phase with respect to the mineral phase. Values of SI greater than, equal to, and less than zero represent, super saturation, equilibrium and under-saturation, respectively for the mineral phase with respect to the aqueous solution. Equilibrium constants for mineral dissolution often vary strongly with temperature. Calcite seems to be close to the super saturation line with few exceptions (Figure 10). In this samples although low calcium concentrations were detected the concentration is expected to equilibrate with time as the well flows and the chemical composition of the deep fluids equilibrates.

PRODUCTION PROPERTIES

Brine handling can be hard in geothermal operations. It is frequently described as the entire periodic table of elements in a pipe. The high temperature solution of elements and compounds, however, causes operational limitations in geothermal power plants. These limitations are due to the severe scaling and corrosion characteristics of geothermal brine and steam. Because of these characteristics, plants may experience extreme plugging and corrosion in wells, lines and equipment. Curtailment in power plant production and even complete plant shutdown are often the end result from these conditions. Different types of brine with differing chemistry conditions are found in various areas around the world. Substantial differences can even be found within the various wells of a given field, just like we have seen in the new Olkaria Domes field. The chemistry of these different brines varies and the differences will depend on several factors including the geology of the resource, temperature, pressure, and water source. Depending on the resource, steam and water ratios in the brine can vary significantly.

The scaling characteristics of brine and steam cause difficult problems in geothermal operation. The variety of problems associated with handling geothermal brine can be extreme – making it critical to understand the chemistry of the brine for successful plant operation. Geothermal brine causes a variety of operational problems and includes the following:

- Equipment Damage and Failure
- Equipment Repair and Replacement
- Well and Line Plugging
- Reduced Steam/Brine Flow
- Power Production Losses
- Complete or Partial Plant Shutdown

The effectiveness of the development of geothermal energy will be determined by the amount of geothermal power that is made available, and this amount will be influenced by the effect that materials problems have on efficiency and downtime. Since every technological effort is limited to some extent by the performance of materials, it is prudent to

consider scaling and corrosion and materials problems which may limit the development of geothermal energy. The availability of durable and cost-effective construction materials for processing geothermal fluids has a definite impact on the development of geothermal energy. Geothermal resources include steam-dominated sources, liquid dominated sources, geo-pressurized sources, and dry (hot rock) sources. Scale is a major problem in geothermal operation. The plugging and deposit problems caused by scale can reduce power plant production, and create expensive cleaning costs. The reduction in power and increased operating costs caused from difficult scale conditions can directly impact a plants financial outcome. Different types of scales are found in various geothermal areas and sometimes, even within the various wells of the same field. The major species of scale in geothermal brine typically include calcium, silica and sulphide compounds. (Stapleton 2002)

To be able find the production properties of the three Olkaria Domes wells, three samples were used to analyse the deep fluid calcite and silica saturation. The species selected for this speciation were those sampled later in the discharge testing period. This was so as to get the close to equilibrium fluids and thus the silica and calcite concentration. The samples selected for silica analysis also had good charge balance and the highest silica concentrations to speciate for the silica deep fluid concentration. The species selected for calcite scaling had the lowest calcium concentration but a representative pH values and CO_2 concentration.

Scaling

Geothermal waters are saturated with silica and are frequently close to saturation with calcite, calcium sulphate and calcium fluoride. Some acid hot water also contains appreciable concentrations of heavy metals. Changes in temperature and pressure disturb the equilibria and will generally lead to scale formation. Calcite and silica deposits are the most frequent scale formation materials. The most troublesome calcite deposits usually occur in the well casing at the level of first boiling (bubble point) with heavy bands of calcite depositing over a short length. (Moller et al, 2004).

Silica scaling

Silica related scale is arguably one of the most difficult scales occurring in geothermal operation. Silica is found in virtually all geothermal brine and its concentration is directly proportional to the temperature of the brine. As brine flows through the well to the surface, the temperature of the brine decreases, silica solubility decreases correspondingly and the brine phase becomes over saturated. When pressure is dropped in the flash vessel, steam flashes and the temperature of the brine further decreases. In the flash vessel, the brine phase becomes more concentrated. Under these conditions, silica precipitates as either amorphous silica or it will react with available cations (e.g., Fe, Mg, Ca, Zn) and form co-precipitated silica deposits.

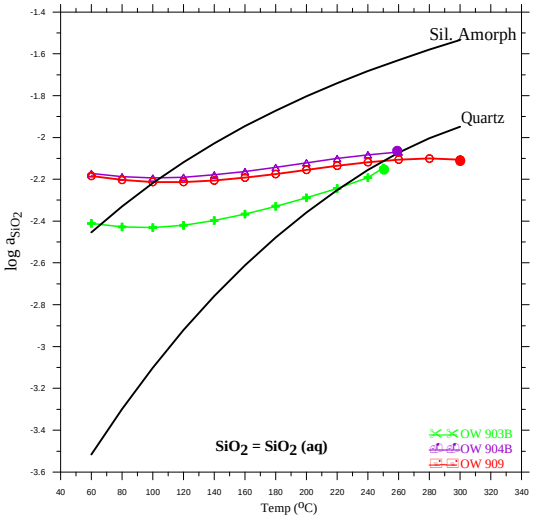

FIGURE 12: Temperatures indicating probable silica scaling in Olkaria Domes.

Scale formation in plant equipment and porosity losses in injection well formations created by the precipitation of amorphous silica have been identified as important problems in some geothermal power operations. In high temperature hydrothermal systems, the formation water is frequently in near equilibrium with quartz. Since the solubilities of pure silica minerals decrease rapidly with decreasing temperature, large amounts of quartz would be expected to precipitate as the brines in these systems are cooled upon production and energy extraction. However quartz rarely precipitates because of the slow kinetics involved in this reaction. Although amorphous silica has a higher solubility than quartz, it is a much more common precipitate in geothermal operations. (Moller et al, 2004). The solubility reactions for silica minerals are invariably expressed in equation (1) and (2).

Since geothermal waters may boil in the upflow of the geothermal system if reservoir temperatures are above 100°C, the boiling causes the concentrations of aqueous solutes to increase in proportion to steam fraction. It also causes the pH of the water to increase because the weak acids dissolved in the water, CO_2 and H_2S, are transferred into the steam phase. To estimate the silica scaling in the new wells drilled in the Olkaria Domes field, WATCH program was used to speciate the analysis and the results indicated on the graphs. From equations 2 and 3 above, $H_4SiO_4^0$ is not the only aqueous silica species in natural waters. $H_4SiO_4^0$ is a weak acid which dissociates, if pH of the fluid is high enough to

yield $H_3SiO_4^-$. Boiling the fluids thus affects the silica concentration leading to the activity of silica to decrease and finally precipitation as amorphous silica at the temperatures shown on the figure 11.

Calcite scaling

Calcite a major scale-forming mineral in many geothermal systems precipitates from a brine according to the following reaction:

$$Ca^{2+}(aq) + 2HCO^-_3 \leftrightarrow CaCO_3(s) \downarrow + H_2O + CO_2 \uparrow \quad (18)$$

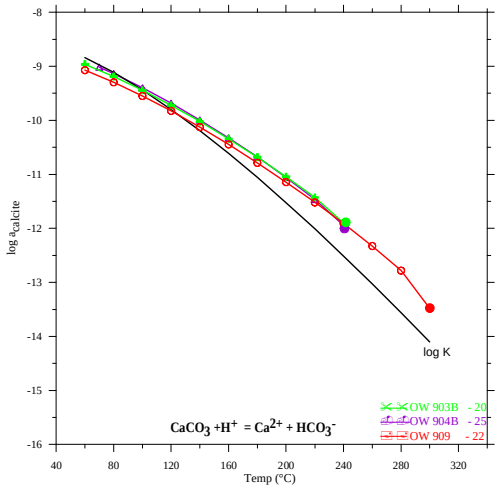

FIGURE 13: Temperatures indicating probable calcite scaling in Olkaria Domes wells.

Ocampo-Diaz et al 2005 found that scale deposition, especially calcite ($CaCO_3$), is a complex function of physical chemistry (for example, total salinity, pH and concentration of calcium and dissolved CO_2) and the pH change upon boiling compared to the rate of cooling upon boiling. Calcite is commonly saturated in the reservoir fluid, and when such fluids boil there is generally a chemical potential to form calcite. However, unlike silica and the sulphides, calcite becomes more soluble as temperature decreases. As result, the most severe calcite scale deposition tends to occur from lower temperature geothermal fluids below 220°C to 240°C.

When reaction 18 is forced to the right by the loss of CO_2 from the liquid phase into a gas phase on flashing, calcite is deposited. In complex brines there may be many other reactions taking place, some of which interact with the calcium and carbonate ions. For this prediction, a sample from each well was selected. The samples selected 20, 25 and 22 for wells OW 903B, OW904B and OW909 respectively had a representative pH and CO_2 with reference to the others from the wells. Although the general calcium concentration is low for these wells, the CO_2 and pH were considered for sample selection. The results from the wells during the initial discharge seemed to have low concentrations of calcium (and high pH values) but trends indicate that with further discharge, the calcium concentrations will increase though not to a great extent. From the WATCH calculations, the calcite saturation is over estimated but considering the deep fluids shown (Figure 12) had been at equilibrium with calcite when the boiling started, then less super saturation would have been experienced during boiling. Calcite scaling will not be a problem in these Domes wells as the low calcium concentrations and high pH, (which affects calcite saturation) indicates.

CONCLUSIONS

- OW 909 seems to have higher concentrations of the cation components as compared to OW 903B and OW 904B. Despite the limited time of recovery, the sulphate concentrations are declining with time as the H_2S concentrations increase showing good geothermal water inflow into the wells.
- Solute and gas geothermometry indicate high temperatures in the range of 250°C to 350°C.
- Olkaria Domes wells have a sodium bicarbonate water type and plot similar to those of Olkaria west and Olkaria central fields. Unlike the wells in the Olkaria East production field and in Olkaria Northeast discharge sodium-chloride type water of mature nature.
- With low calcium concentrations and high pH, calcite scaling can be expected to be minimal in these wells but fluid has to be separated at temperatures above 100°C to prevent silica scaling. There´s also low carbon dioxide emission from these wells.

ACKNOWLEDGEMENTS

I would like to extend my sincere gratitude to Dr. Ingvar B. Fridleifsson, the Director of the UNU Geothermal Training Programme for giving me the chance to take part in the Programme, and to the Deputy Director Lúdvík S. Georgsson for his ever present help. To Thorhildur Isberg for her essential and valuable assistance during my stay in Iceland. To Dorthe Holme and Markus Wilde for their expertise in making the studies and project work go easy.

My great and sincere appreciation to my project supervisor Dr. Thrainn Fridriksson (ISOR, Iceland) for his ever present guidance and hand in each page of this project paper. For his wise counsel, encouragement and efficiency in the supervision of this project paper. To the 2009 UNU fellows who were always supportive and the friendships forged. To the entire Orkustofnun community, thank you for all the assistance and support. I am grateful to the Kenya Electricity Generating Company, for the data from the geothermal wells and the opportunity to study the Olkaria Domes field. A big thank you to Kizito Opondo for updating me with geochemical data. To my parents, Dr & Mrs W.O. Wanyanga, for their love, support and encouragement. Finally, to God the Almighty for granting me the wisdom and guidance always.

REFERENCES

Ármannsson, H. and Ólafsson, M., 2006: Collection of geothermal fluids for chemical analysis. Iceland GeoSurvey-ÍSOR, Reykjavík report ISOR-2006/016, 17 pp.

Arnórsson S., 1998: Interpretation of chemical and isotopic data on fluids discharged from wells in the Momotombo geothermal field with notes on gas chromatography analysis, IAEA Project report NIC/8/008-05, 28 pp.

Arnórsson, S. and Bjarnason, J.Ó., 1994: Icelandic Water Chemistry Group presents the chemical speciation programme WATCH Program upgrade: Version 2.1. Science Institute, University of Iceland, Orkustofnun, Reykjavík, 7 pp.

Arnórsson, S. and Gunnlaugsson, E., 1983: Gas chemistry in geothermal systems. Proceedings of the 9th Workshop on Geothermal Reservoir Engineering, Stanford University, Stanford, California, 231-237.

Arnórsson, S., Gunnlaugsson, E., and Svavarsson, H., 1983: The chemistry of geothermal waters in Iceland II. Mineral equilibria and independent variables controlling water compositions. Geochim. Cosmochim. Acta, 47, 547-566.

Clarke, M.C.G., Woodhall, D.G., Allen, D., and Darling, W.G., 1991: Geological, volcanological and hydrogeological controls on the occurrence of geothermal activity in the area surrounding Lake Naivasha, Kenya. Ministry of Energy, Nairobi, Kenya, report, 138 pp. + 3 maps.

D'Amore, F. and Arnórsson, S., 2000: Geothermometry. In: Arnórsson, S.(ed.), Isotopic and chemical techniques in geothermal exploration, development and use. Sampling methods, data handling, and interpretation. International Atomic Energy Agency, Vienna, 152-199.

D'Amore, F. and Celati, C., 1983: Methodology for calculating steam quality in geothermal reservoirs. Geothermics, 12. 129-140.

D'Amore, F., and Truesdell, A.H., 1985: Calculation of geothermal reservoir temperatures and steam fractions from gas compositions. Geothermal Resources Council, Trans., 9, 305-310.

Fournier, R.O., 1977: Chemical geothermometers and mixing model for geothermal systems. Geothermics, 5, 41-50.

Fournier, R.O., 1979: A revised equation for the Na/K geothermometer, Geotherm. Resources Council Trans., 3. 221 -224.

Fournier, R.O. and Potter, R.W.II., 1982: A revised and expanded silica (quartz) geothermometer. Geoth. Res. Council, Bull., 11-10, 3-12.

Giggenbach, W.F., 1988: Geothermal solute equilibria. Derivation of Na-K-Mg-Ca geoindicators. Geochim. Cosmochim. Acta, 52, 2749-2765.

Giggenbach, W.F., 1991: Chemical techniques in geothermal exploration. In: D'Amore, F. (coordinator), Application of geochemistry in geothermal reservoir development. UNITAR/UNDP publication, Rome, 119-142.

Karingithi, C.W., 2000: Geochemical characteristics of the Greater Olkaria geothermal field, Kenya. Report 9 in: Geothermal Training in Iceland 2000. UNU-GTP, Iceland, 165-188.

Lagat, J.K., 2004: Geology, hydrothermal alteration and fluid inclusion studies of the Olkaria Domes geothermal field, Kenya. University of Iceland, MSc thesis, UNU-GTP, Iceland, report 2, 71 pp.

Moller, N., Greenberg, J.P., Weare, J.H., 2004: Computer modelling for geothermal systems: predicting carbonate and silica scale formation, CO2 breakout and H2S exchange. Transport in Porous Media Journal, 33-1/2. 173-204.

Mungania, J., 1992: Surface geology of Olkaria- Domes field. Kenya Power Company, unpublished internal report.

Mungania, J., 1999: Reservoir model of Olkaria- Domes field. KenGen, unpublished internal report.

Ocampo-Díaz J.D., Núñez, Q.M., Moya-Acosta, S.L., 2005: Silica scaling as a predominant factor of the production in Cerro Prieto geothermal wells, Mexico. Proceedings of the World Geothermal Congress 2005, Antalya, Turkey, 5pp.

Omenda, P.O., 1999: Borehole geology of Well OW-901. KenGen, unpublished internal report.

Onacha, S.A., 1993: Resistivity survey of Olkaria- Domes field. Kenya Power Company, unpublished internal report.

Onacha, S.A., and Mungania, J., 1993: Surface exploration of Domes Area: An extension of Olkaria Geothermal Field. Proceedings of the 14th New Zealand Geothermal Proceedings, Auckland, NZ. 6 pp.

Opondo, K.M., 2008: Fluid characteristics of three exploration wells drilled at Olkaria Domes field, Kenya. Proceedings of the 33rd Workshop on Geothermal Reservoir Engineering, Stanford University, Stanford, Ca, 6 pp.

Pang Z.H., and Ármannsson, H. (editors), 2006: Analytical procedures and quality assurance for geothermal water chemistry. UNU-GTP, Iceland, Report 1, 172 pp.

Stapleton, M., 2002: Scaling and corrosion in geothermal operation. GeoChemical Services - PowerChem Technology. 7 pp.

Tole, M.P., Ármannsson, H., Pang Z.H., and Arnórsson, S., 1993: Fluid/mineral equilibrium calculations for geothermal fluids and chemical geothermometry. Geothermics, 22, 17-37.

Appendix I

Water and Gas analysis

	OW 903B Water Analysis (ppm)																		Gas Analysis (ppm)				
Day	GSP	WHP	Temp	Enth. kJ/kg	Cond	TDS (ppm)	pH	B	SO_4	Cl	CO_2	F	H_2S	SiO_2	Ca	Li	Na	K	Mg	CO_2	H_2S	CH_4	H_2	N_2
1	2.1	3.8	94.0	1307	2776	1390	9.5	0.9	717.7	196.7	266.2	41.6	0.1	281.3		1.5	512.6	55.1	0.7	4382	9.2	15.8		418
2	2.3	3.8	90.0	1325	2924	1462	9.4	0.1	699.0	175.7	225.3	46.5	0.3			1.4	482.3	61.6	0.2		3.2	15.0	0.2	2033
3		4.0	94.5	1466	2740	1368	8.7	1.7	677.6	178.2	436.7	45.6	0.2	285.3			549.6	71.6		4580	4.0	27.6	0.2	1980
9		4.0	90.0	1516	2310	1156	9.6	1.8		202.0	243.3	43.8	1.2	287.5		1.4	498.5	83.8		5091	11.9	41.8		1273
10	2.3	3.8	89.5	1425	2967	1481	9.6	0.1	679.4	189.6	290.4	58.0	1.0	184.5	3.6	1.4	589.2	80.8		6189	2.8	0.2		16
13	1.8	3.6	89.0	1567	2954	1490	10.2	0.6	497.2	201.6	341.0	50.4	1.7	251.8	8.3	1.2	538.4	90.7		5221	42.4	8.0	0.3	764
14	1.2	3.6	92.0	1595	2968	1525	9.5	0.7	472.2	203.1	385.9	55.8	1.4		0.7	1.2	564.7	82.8		8080	5.5	5.6	0.2	452
15	3.4	5.2	89.0	1461	2993	1497	9.6	0.9	639.4	199.5	281.1	51.2	3.4	266.3		1.6	535.8	94.8		5227	9.4	18.9	1.8	1603
16	3.7	5.7	85.0	1434	2942	1471	9.5	1.0	708.1	224.7	303.4	60.4	0.7	413.0		1.4	513.3	92.2			1.3	9.8	0.9	678
17	4.1	7.5	84.1	1334	2870	1431	10.1	0.8	655.2	195.6	330.0	50.0	2.4		0.1	1.1	482.7	49.7			7.2	9.5	0.9	664
20	4.1	7.6	86.0	1253	2897	1422	9.4	0.7	624.8	202.4	338.4	64.0	0.5	585.0	1.6	1.2	411.5	87.0		5753	7.0	7.0	0.7	469
21	3.8	7.9		1453	2897	1442	9.6	0.2	538.2	220.8	280.5	53.8	1.0	273.5	1.6	1.5	431.9	0.0						
24	4.1	7.6	85.0	1247	2880	1450	9.2	1.0	446.4	211.6	274.2	66.5	1.2	250.0	1.5	1.5	571.7	94.0		12788	10.9	27.6	0.7	465
30	4.1	7.2	88.0						380.8						7.2									
35	3.8	5.9	93.0	1007			10.2	0.4	481.1	224.0	273.5	79.0	0.7	304.5	1.5	0.0	526.5	105.1		6665	11.3	1.3	0.4	480
43	3.4	5.6		1916	2966	1483	10.1	1.3	418.0	220.0	322.3	67.5	0.9	677.0	1.0	2.9	533.0	112.1		11275	2.4	4.9	42.6	17
50	3.4	4.8		1591	2954	1477	9.5	1.3	310.0	243.0	351.1	73.0	0.7	627.0	1.0	1.2	483.1	95.7		14197	2.3	2.7		12
58	2.1	3.8		1307	2775	1390	9.5	0.9	718.0	197.0	317.0	42.0	0.1	281.0	1.9	1.5	717.0	55.0	0.7	4383	9.3	95.6	29.8	
62	3.9	6.2		1490	2887	1444	10.3	2.2	336.0	252.0	348.0	82.0	1.9	621.0	1.2	1.2	614.0	124.0		3396	33.4	1.5	26.2	9
64	4.1	6.3		1414	2980	1488	9.4	2.7	333.0	252.0	359.0	75.0	1.5	649.0	0.3	1.9	634.0	106.0		4146	99.9	1.8	26.3	9
70	3.4	6.2		1638	2880	1450	9.6	2.3	306.0	209.0	365.0	80.0	4.8	499.0	0.6	2.8	628.0	127.0		3941	267.7	1.1	16.8	6
72	4.6	8.3		1487	2906	1455	9.7	2.5	350.0	281.0	383.0	59.0	4.8	587.0	0.1	0.1	613.0	138.0		4292	144.6	0.9	16.9	
79	4.1	8.1		1535	2945	1472	9.9	2.3	323.0	262.0	362.0	77.0	5.0	449.0	0.2	4.7	612.0	124.0		4229	29.1	4.4	39.4	8
84	5.5	10.3		1466	2842	1421	10.1	2.2	310.0	267.0	374.0	62.0		726.0	0.3	2.6	612.0	129.0		9604	120.6	2.8	16.0	7
86	2.8	10.3		1488	2902	1451	9.9	2.0	278.0	587.0	360.0	61.0	5.8	623.0	1.2	0.2	620.0	139.0		10134	32.2	3.4	22.3	10

	OW 904B Water Analysis (ppm)																		Gas Analysis (ppm)				
Day	GSP	WHP	Temp	Enth. kJ/kg	Cond	TDS (ppm)	pH	B	SO_4	Cl	CO_2	F	H_2S	SiO_2	Ca	Li	Na	K	Mg	CO_2	H_2S	CH_4	H_2	N_2
1	2.1	3.2	94.0	1307	2222	1106	6.0		782.5	124.3		36.8	3.4	212.0		0.4	322.0	52.9	0.5		3.4			
3	3.6	7.9	87.0	1325	2183	1092	5.7	1.4	686.1	124.6		48.9	0.4	106.5		0.5	298.5	19.2	0.5	9166	8.6	45.0	2.4	3570
4	2.4	4.0	90.0	1466	2090	1045	5.9	1.0	732.2	133.5	172.6	49.1	0.2	238.8			359.0	48.4		10034	6.4	20.7	2.3	869
10	2.4	5.0	90.0	1516	3085	1540	8.8	0.9	591.2	177.1		49.4	0.2	207.7	3.4	0.8	347.3	46.3		8719	36.7	143.1	1.4	420
14	2.8	4.6	89.0	1567	2061	1037	9.7	0.9	401.6	168.3	337.9	61.8	0.8	285.7	1.1	0.6	350.7	42.4		8248	2.1	14.5	6.3	984
15	2.8	4.9	89.0	1595	2275	1137	9.1	1.0	515.3	182.8	171.6	51.8	1.4	0.0	2.0	0.9	434.3	45.0		21770	1.9	19.5	7.3	1090
16	4.4	6.5	83.0	1461	2286	1143	9.2	0.3	562.9	198.8	124.9	50.1	3.4	243.0		0.9	446.2	47.3		13084	13.0	29.4	3.7	1042
17	5.1	6.5	81.3	1434	2253	1126	9.2	0.5	556.1	203.8	171.8	59.1	0.5	326.0		0.8	419.4	45.0		4359	8.2	37.0	4.6	1270
18	5.0	6.9	85.0	1334	2259	1129	10.0	0.1	647.2	192.8	255.4	52.2	0.3	0.0	1.0	0.4	413.9	47.2		21677	26.5	32.7	3.7	1051
21	5.0	6.7	84.0	1253	2203	1102	9.4	1.0	524.1	198.4		52.3	0.3	546.0	1.8	1.0	350.6	46.6		10421	5.8	34.4	3.9	1094
24	4.5	6.7	84.0	1471	2031	1010	9.6	2.0	160.0	207.0	144.6	62.0	5.8	621.0	3.1		428.2	52.0		8993	15.6	29.9	3.8	846
25	5.1	6.9	85.0	1525	2271	1139	9.4	0.2	429.6	178.6	156.9	60.6	2.2	625.0	2.3	0.5	497.8	44.6		14065	13.5	31.5	4.3	1190
31	5.0	6.5			2894	1138	9.5	0.2	381.2	200.6	199.3	55.3		247.5	2.8		408.1	49.8		199				
36	3.6	5.4		1676			10.0	1.5	414.0	213.0	197.6	50.8	1.4	220.0	0.2		421.9	48.5		9525	8.9	3.5	10.3	362
44	3.5	6.2		1560	2366	1183	9.7	2.1	289.6	209.5	237.6	57.6	1.3	516.0	1.0	1.4	426.2	51.1		12243	120.6	3.8	20.7	136
51	4.1	5.2		2178	2390	1196	9.7	1.2	277.5	216.7	265.5	57.7	1.4	175.0	1.4	1.3	479.9	56.8		12744	6.3	3.4	23.0	103
58	3.5	7.6		1824	2350	1181	9.6	2.7	278.4	226.4	330.0	73.5	1.4	420.0	1.0	1.2	500.1	64.0		7937	2.5	3.0	22.2	311
63	3.9	7.6		2009	2341	1169	10.3	2.4	241.4	240.2	253.0	54.0	2.8	492.0	0.6	1.2	489.6	62.6		6458	74.6	6.8	3.4	337
65	4.3	7.2		2043	2376	1199	9.4	2.0	244.2	240.5	276.5	54.3	4.8	559.0	0.9	1.2	487.3	60.3		6240	28.3	6.3	2.3	
71	6.9	9.7		1535	2062	1029	9.8	2.1	217.9	186.7	290.8	50.6	8.2	446.0	0.7	1.1	460.8	78.3		5631	164.9	7.8	2.3	370
73	7.6	10.3		1690	2386	1193	9.7	1.7	232.4	255.0	294.4	53.5	8.1	677.0	0.7	0.9	454.9	71.8		7735	135.6	6.9	2.2	331
80	5.4	10.3		1481	2380	1190	10.0	1.8	214.7	227.0	262.9	57.9	9.5	502.0	0.7	1.1	457.3	76.7		9418	77.7	5.1	2.0	321
85	5.5	17.9		1812	2295	1147	10.2	2.0	189.1	231.3	290.2	54.4	8.5	652.0	1.1	1.2	459.1	87.6		12541	271.1	13.5	5.7	283
87	5.2	17.9		2168	2366	1182	9.9	1.9	208.0	249.0	275.9	53.2	7.8	758.0	0.8	1.1	455.0	128.1		21428	177.9	10.4	5.3	338
92	5.5	17.0		1924	2287	1143	9.7	2.8	193.1	247.9	286.9	54.1	8.2	479.0	0.3	1.1	495.1	142.5		10159	160.7	13.7	6.3	289
94	2.9	17.9		1857	2298	1140	9.6	3.0	206.5	303.6	278.1	52.9	6.9	473.0	1.4	1.2	455.9	131.1		8396	210.7	16.0	8.8	851

Water and Gas analysis (Cont)

	OW 909 Water Analysis (ppm)																	Gas Analysis(ppm)				
Day	GSP	WHP	Temp	Enth. kJ/kg	Cond	TDS (ppm)	pH	B	SO_4	Cl	CO_2	F	H_2S	SiO_2	Ca	Li	Na	K	CO_2	H_2S	CH_4	H_2	N_2
1	3.7	2.8	86.0	1552	3910	2737	9.6	0.1	177.3	652.8	294.4	229.0	0.3	358.0	1.6	0.4	779.0	215.7	8710.2	5.4	0.0	1.1	3188.0
5	3.1	6.2	89.0	2001	4000	2800	10.1	0.6	250.3	732.4	203.1	250.0	1.0	530.0	2.6	0.4	641.7		11302.9	2.8	2.3	12.3	380.1
8	2.9	6.9	86.0	1697	3999	2000	9.9	0.1	152.6	743.4	162.8	284.9	1.4	395.0	6.6	0.3	732.4	222.5	162.8	1.4	0.0	0.0	0.0
9	3.4	6.5	90.0	1875	4230	2961	9.4	0.4	179.8	765.7	202.8	323.6	1.2	652.0	0.4	0.4	852.9	255.5	3983.4	5.5	1.0	15.9	223.5
14	3.4	6.2		1904	4350	3045	10.0	1.0	85.0	772.3	275.7	310.7	0.3	436.5	0.4	1.9	770.0	270.7	5386.6	0.9	1.2	29.6	414.1
16	3.4	7.0		1783	4430	3101	9.8	0.6	109.4	875.4	255.4	305.5	0.5	441.0	0.1	0.3	869.1	274.2	4116.5	2.7	1.3	26.9	375.6
19	2.2	3.6		1831	4450	3115	10.0	0.0	0.0	827.9	230.6	235.0	0.3	943.0	0.3	0.4	900.0	260.4	9347.8	5.6	0.0	0.0	0.0
21	3.5	7.0		1696	5420	2711	10.3	2.9	81.2	817.6	179.1	292.4	0.7	932.0	0.2	2.8	850.8	304.3	13494.2	12.5	1.8	32.9	68.4
22	3.5	7.0		1990	5032	2516	10.0	2.7	69.9	786.6	218.7	257.4		898.0	0.2	2.0	913.4	287.4	6479.0	7.0	1.1	28.9	32.4
23	3.0	7.0		2220	6168	3100	10.1	2.2	95.8	803.7	261.6	191.9		738.0	0.2	2.8	905.8	280.2	13937.0	4.9	1.0	24.9	23.0
26	3.1	7.0		2051	2223	1104	10.0	1.6	132.3	780.5	255.0	287.8	0.5	950.0	0.5	1.1	909.3	286.0	8735.3	12.0	1.0	27.0	31.0
27	3.5	6.3		2015	3999	2000	9.6	3.3	116.7	803.6	226.8	263.9	0.7	598.0	0.1	0.4	954.4	270.0	12924.5	10.6	0.7	20.0	15.4
28	3.5	6.3		2070	4972	2486	10.0	3.9	116.6	806.8	248.2	249.0	0.5	664.0	0.2	2.7	954.0	274.6	7409.8	4.8	1.1	20.6	247.9
29	3.3	6.3		2050	2316	1155	10.0	3.5	115.6	822.0	230.6	261.7	0.3	831.0	0.2	2.1	962.6	374.6	5364.8	3.5	9.8	3.6	413.1
30	4.0	7.0		2028	4480	2000	9.8	2.5	112.5	812.3	266.9	264.5	0.7	812.0	0.1	0.2	950.2	357.8	14369.4	2.1	12.1	38.9	544.6
33	3.9	6.9		2029	4490	2000	10.0	2.7	114.2	810.9	289.7	250.7	0.7	760.0	0.1	6.6	939.2	398.3	2937.6	6.0	6.4	3.0	284.8
35	3.7	6.9		1955	4712	2358	9.9	5.9	88.2	810.2	232.3	244.9	0.7	693.0	0.2	6.1	903.3	388.5	4255.7	2.4	6.2	2.6	279.2
40	3.5	5.7		2273	5348	2674	10.6	3.3	83.7	816.1	202.2	270.3	0.9	950.0	0.1	2.2	925.5	360.3	7665.0	21.8	5.5	0.4	448.7
42	3.5	6.5		1834	5858	2929	10.3	4.7	82.4	849.2	216.7	287.1	2.4	645.0	0.2	0.0	909.6	373.1	3572.9	287.5	9.6	3.8	282.3
48	3.2	6.6		2089	9750	3750	10.1	5.8	62.6	682.5	294.1	236.7	0.9	769.0	0.3	6.2	893.6	396.5	3393.2	30.4	9.6	18.1	53.9
50	3.3	6.5		2065	5360	2690	10.0	4.1	46.1	847.1	280.3	263.9	3.1	965.0	0.2	7.3	863.9	387.6	3483.6	22.1	7.5	3.3	214.2
57	4.1	7.9		1985	5192	2598	10.2	4.6	46.9	822.2	183.5	259.7	3.0	500.0	0.2	2.0	911.0	380.4	5725.9	50.0	5.1	2.3	208.5
62	4.1	8.0		1993	4656	2328	10.3	2.2	51.6	843.0	265.0	273.2	1.2	886.0	0.1	1.3	912.1	434.1	4840.7	55.8	8.8	6.2	161.6
64	5.2	8.1		1991	4825	2420	10.2	4.7	42.7	719.5	286.2	272.0	3.4	926.0	0.1	6.0	892.9	340.2	8309.6	53.1	8.9	6.0	133.0
69	4.5	8.3		2016	4794	2398	10.0	5.0	38.9	872.7	222.4	289.8	3.4	835.0	0.7	2.8	951.6	281.5	4851.9	7.7	12.0	7.8	87.5
71	2.6	8.5		2235	2364	1181	9.8	4.7	41.6	836.4	245.7	230.7	3.4	443.0	0.3	1.1	974.1	363.2	3441.6	63.1	25.5	19.2	623.5
78	1.8	8.4		2150	5175	2550	9.9	4.6	25.8	836.4	251.7	226.0	3.4	569.0		1.4	942.7	165.3	4761.6	58.9	0.9	2.0	115.4
84	3.1	8.5		1996	4524	2260	10.5	4.6	47.4	936.0	184.4	230.2	3.4	716.0		2.7	1047.0		3942.0	72.3	13.4	3.5	674.2
85	3.7	8.4		2153	3243	1623	10.1	4.1	26.0	853.7	237.8	263.2	3.0	746.0		2.7	1003.0		6011.4	31.6	16.6	6.3	113.2
90	7.0	10.4		2168	5302	2651	10.6	4.3	47.2	848.9	170.9	257.9	2.9	884.0		2.9	995.0		6672.4	46.2	9.0	3.9	83.7
92	4.8	10.0		2219	4364	2680	9.9	4.7		591.3	199.3	235.0	3.7	725.0		3.0	1056.0		5314.3	74.6	2.9	1.3	165.3
97					5378	2689	10.3	3.3	50.7	824.7	244.0	244.0	2.7	512.0		2.9	807.5		4780.6	61.6	0.2	0.5	88.1
104	5.4	14.3		1527	6420	3210	10.7	3.4	7.7	545.3	213.0	305.2	2.8	831.0		3.0	734.0		6163.2	38.1	1.1	2.5	267.2
106	4.8	14.3		2072	4320	2200	10.5	3.8	24.5	545.3	192.1	260.9	3.0	583.0		2.9	1040.0		4186.4	14.9			132.4
112	5.2	23.1		1872	4980	2490	11.0	3.7	27.5	812.1	165.2	307.6	2.4	703.0		3.0			165.2	2.4			
118				1994			11.0	3.8	21.3	799.2	147.4	255.6		560.0		3.0			147.4				
121	1.7	7.2		1232			10.9																

Deep fluid concentrations

Well/Sample No.	pH	B	SiO_2	Na	K	Mg	Ca	F	Cl	SO_4	TDS	CO_2	H_2S	H_2	CH_4	N_2
903B - 13	7.0	0.7	176.2	402.8	66.2	0.0	1.1	46.9	149.1	314.5	1021.7	1239.6	1.7	0.1	2.3	38.1
903B - 18	7.5	0.6	198.0	505.2	38.8	0.5	1.3	29.6	138.8	505.9	979.4	585.9	0.8	2.5	7.9	0.0
903B - 20	7.7	1.9	457.3	446.7	74.7	0.0	0.2	52.8	177.6	234.6	1048.4	592.2	9.2	2.2	0.1	0.7
903B - 21	7.8	1.6	351.6	442.5	89.5	0.0	0.4	56.4	147.3	215.6	1021.7	580.8	25.4	1.4	0.1	0.5
904B - 11	7.2	1.4	424.0	292.4	35.5	0.0	2.1	42.3	141.3	109.3	689.6	991.3	5.0	0.4	3.0	85.4
904B - 12	6.9	0.1	426.8	339.9	30.5	0.0	1.6	41.4	122.0	293.3	777.7	1510.0	2.6	0.4	3.2	120.1
904B - 16	7.0	0.8	119.5	327.7	38.8	0.0	1.0	39.4	148.0	189.5	816.6	1443.9	1.5	2.3	0.3	10.4
904B - 19	7.4	1.4	381.7	332.7	41.2	0.0	0.6	37.1	164.2	166.7	818.7	792.2	5.7	0.2	0.6	0.0
904B - 24	7.1	1.3	517.6	310.7	360.6	0.0	0.6	36.3	170.0	142.0	807.1	2321.9	22.5	0.5	1.0	34.1
904B - 25	7.3	1.9	327.1	338.1	97.3	0.0	0.2	36.9	169.3	131.9	780.5	1191.7	21.0	0.6	1.4	29.2
909 - 12	7.3	1.9	352.7	562.8	159.2	0.0	0.1	155.6	473.9	68.8	1179.0	1962.3	1.8	2.9	0.1	2.2
909 - 15	7.4	1.5	478.9	560.4	211.0	0.0	0.1	156.0	479.0	66.3	1179.5	2188.3	0.6	5.6	1.7	78.4
909 - 17	8.0	3.5	408.7	532.7	229.1	0.0	0.1	144.4	477.8	52.0	1390.6	718.1	0.7	0.4	0.9	40.3
909 - 20	8.3	3.4	453.5	527.0	233.8	0.0	0.2	139.6	402.5	36.9	2211.5	624.8	4.9	2.6	1.4	7.9
909 - 22	7.8	2.7	294.9	537.5	224.3	0.0	0.1	153.2	484.9	27.7	1532.1	912.3	8.6	0.3	0.7	30.0
909 - 26	7.9	2.8	261.3	574.5	214.2	0.0	0.2	136.0	493.2	24.5	696.5	609.1	10.7	2.8	3.7	90.6

Appendix II

Trends in the discharge contents of Olkaria Domes wells

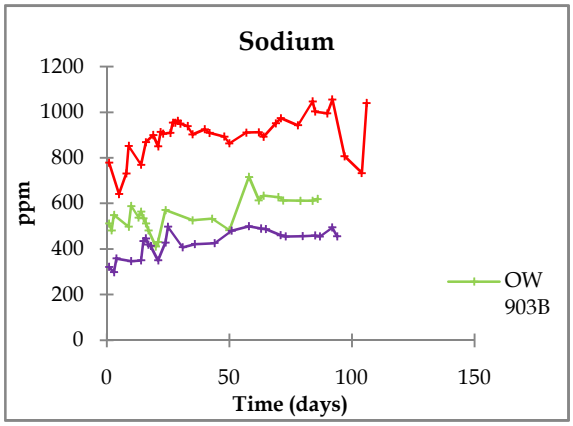

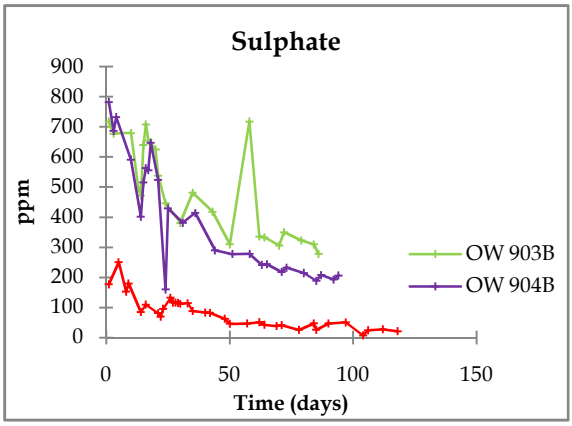

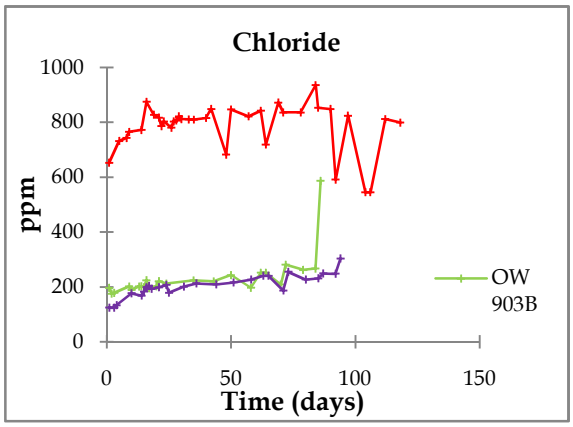

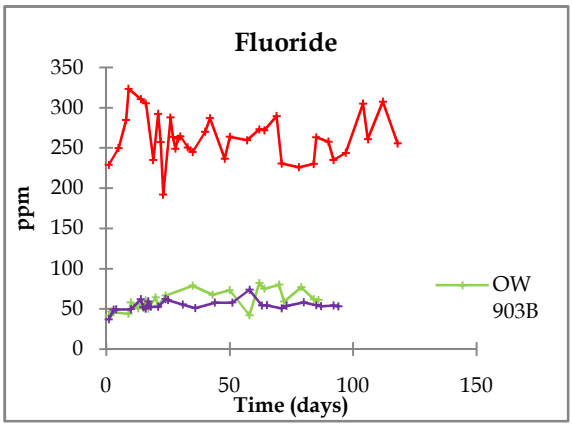

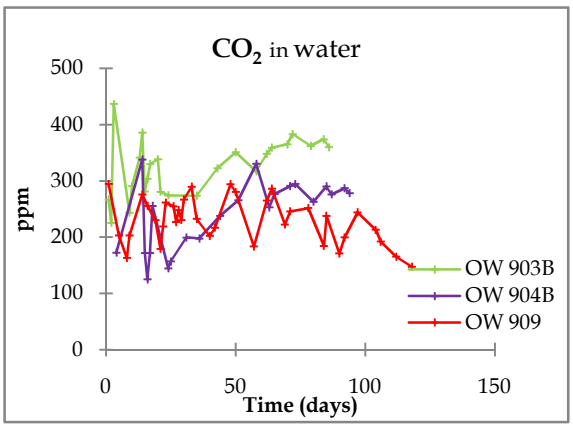

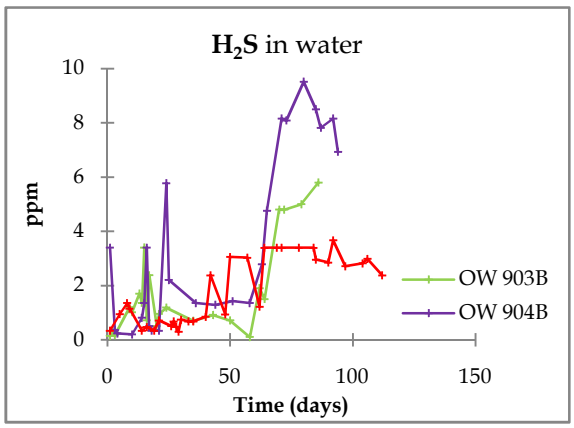

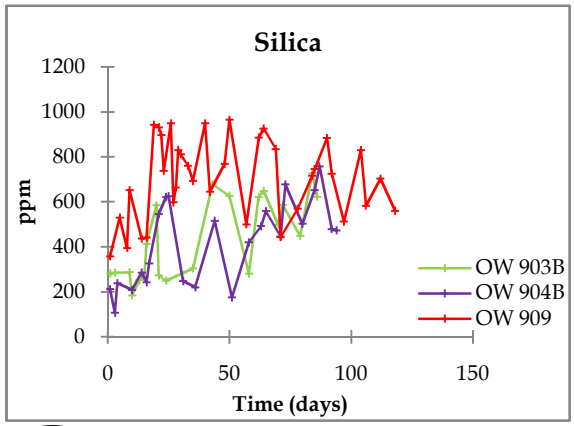

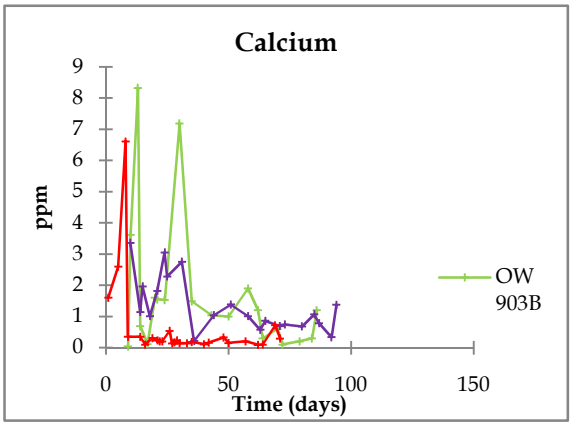

Trends in the discharge contents of Olkaria Domes wells (Cont.)

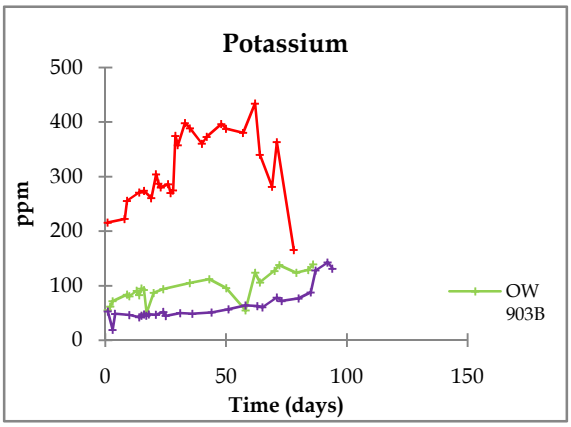

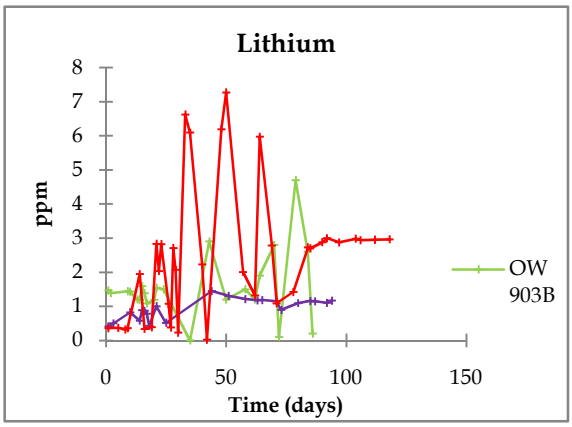

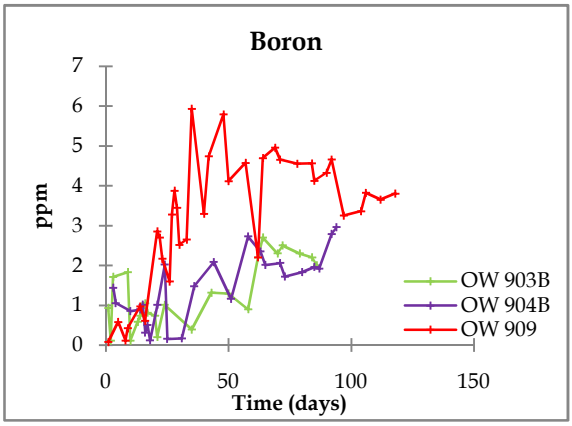

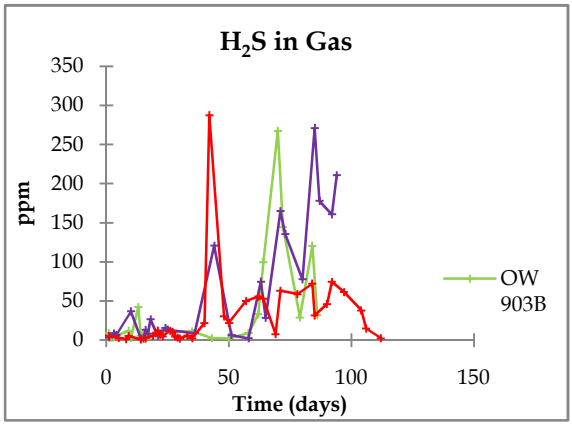

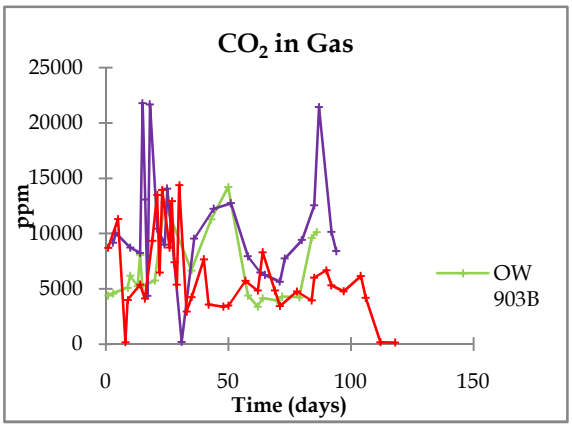

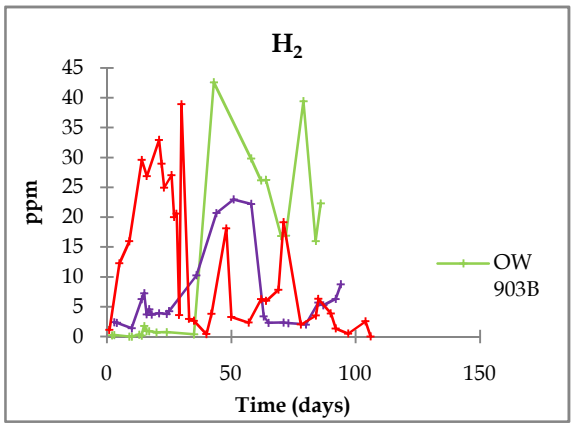

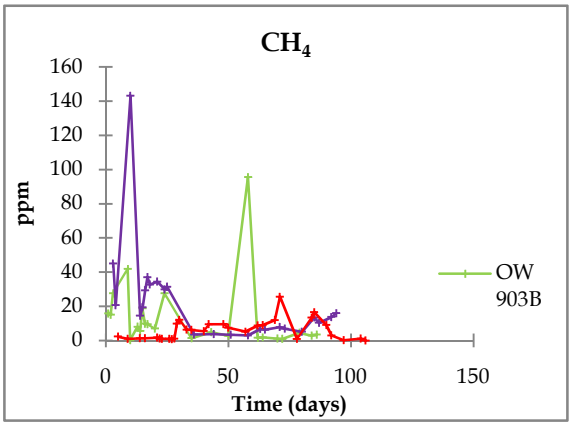

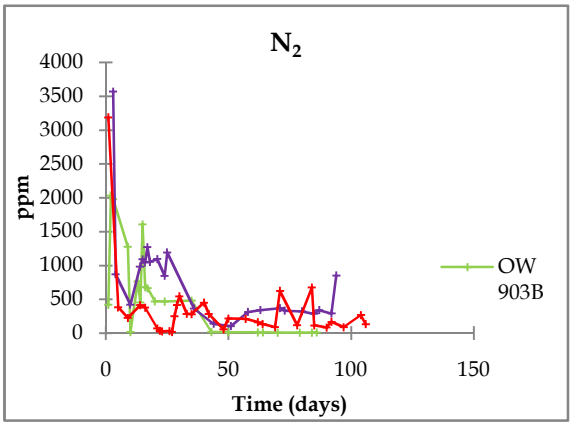

Appendix III

Deep fluid chloride correlation with other elements.